

CRYSTAL STRUCTURE OF β' PHASE IN AN Al-1.0mass%Mg₂Si ALLOY

Kenji Matsuda¹, Shizuo Tada¹, Susumu Ikeno², Tatsuo Sato³ and Akihiko Kamio³

1: Department of Engineering, Toyama University, 3190, Gofuku, Toyama, 930, Japan.

2: Center for Cooperative Research, Toyama University, 3190, Gofuku, Toyama, 930, Japan.

3: Department of Metallurgical Engineering, Tokyo Institute of Technology, O-okayama, Meguro-ku, Tokyo, 152, Japan.

Abstract

The crystal structure of the rod-shaped β' phase in an aged Al-1.0mass%Mg₂Si alloy was investigated by the diffraction patterns, high resolution images and energy dispersive X-ray spectra. According to the present results, the crystal structure of this phase is proposed as follows: The crystal system is H.C.P. having $Mg/Si=1.68$ and its lattice parameters are $a=0.407nm$ and $c=0.405nm$.

Introduction

Al-Mg₂Si alloys have been investigated as the prominent materials for vehicles instead of steel in Japan[1]. It has been known that the metastable β' phase in Al-Mg-Si alloys precipitated by aging is rod-shaped lying along $\langle 100 \rangle$ matrix directions [2,3]. The crystal system of the β' phase had been reported to be a F.C.C by Thomas[2] or a hexagonal by Jacobs [3], but accurate crystal structure has not yet been clarified. The β' phase is possibly assumed to have a composition of $Mg:Si=2:1$ based on the equilibrium phase diagram. There are no reports analyzing the chemical compositions of the β' phase. We have obtained new results on the β' phase in an Al-1.0mass%Mg₂Si alloy by using an HRTEM (high resolution transmission electron microscope)[4]. The shape of the transverse cross section of the β' phase is ellipsoidal with its longer diameter elongated along the specific direction of the matrix. The analysis of the micro-beam diffraction patterns was in good agreement with the proposed crystal system by Jacobs [3]. But we could not identify the crystal structure of the β' phase because of the absence of various electron diffraction patterns taken from different directions of the β' phase. In addition, because of the lack of detailed examinations for the intensity and coordinate of diffraction spots the positions of the constituent atoms could not be determined.

In this study, we attempted to obtain the electron diffraction patterns for the parallel and normal directions to the rod-shaped β' phase in an Al-1.0mass%Mg₂Si alloy in order to determine the crystal structure. The diffraction patterns were analyzed based on the orientation relationship between the matrix and the β' phase[4], and also the patterns were compared with those calculated by the computer simulation. High resolution (H.R.) images were calculated based on the determined crystal structure and were compared with the actual

were calculated based on the determined crystal structure and were compared with the actual H.R. images. Furthermore, the chemical compositions of the β' phase was analyzed by the energy dispersive X-ray (EDX) spectrometer. The results suggested that the chemical compositions of the β' phase are somewhat different from stoichiometric ratio, Mg:Si=2:1.

Experimental

The Al-1.0mass%Mg₂Si alloy was prepared using 99.99mass% aluminium, 99.9mass% magnesium and 99.9mass% silicon ingots. These were melted in air and solidified in steel mold. This obtained ingot was rolled to 0.2mm thick sheets. These sheets were heated at 848K for 3.6ks in air for the solution heat treatment and quenched in cold water. The aging treatment was at 523K for 12ks in a salt bath, the aging time being equivalent to obtain the maximum hardness[5]. The aged specimens were electrolytically polished for the transmission electron microscope(TEM) observation. A HRTEM observation was performed with an EM-002B type electron microscope (TOPCON Co.,Ltd.) equipped with EDX spectrometer (EDAX Inc.). A TEM of JEOL 2000FX-II equipped with a double tilt specimen holder was also used to tilt specimens to higher angles than 20 degrees.

Results and Discussion

Electron diffraction

Figure 1(a) is a bright field image of the specimen aged at 523K for 12ks. The incident beam is parallel to the [001] matrix direction and the longitudinal directions of the β' phase are parallel to the [100] and [010] matrix directions. Therefore, the dark colored precipitate particles are the cross sections of the rod-shaped β' (hereafter called as rod-sections). Figure 1(b) is an example of the H.R. images of the rod-sections. The shape of the rod-section is ellipsoidal, being elongated toward the [010]m direction.

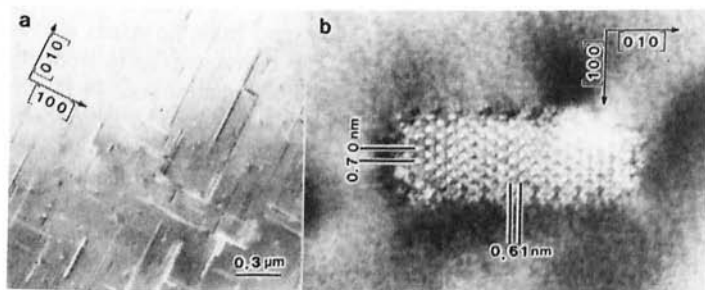


Figure 1. A bright field image of the specimen aged at 523K for 12ks (a) and an example of the H.R. images of the rod-sections of the precipitates (b).

Figure 2(a) shows the MBD pattern obtained from the rod-section. Both the diffraction spots from the matrix and the hexagonal network of the diffraction spots from the rod-section can be seen in Fig.2(a). Fig.2(d) is a schematic illustration of Fig.2(a). In the figure, the plane spacing between 000 transmitted spot and the nearest diffraction spot is about 0.61nm. If the crystal

system of the unit cell of the β' phase is a hexagonal and the size of a-axis is $a=0.705\text{nm}$ [3], the spacing of 0.61nm corresponds to the plane spacing of $\{\bar{1}\bar{2}10\}_p$ plane. Based on this result, $[\bar{1}\bar{2}10]_p$ of the β' phase is expected to be parallel to $[100]_m$ direction in the case of Fig.2(a). Figure 2(b) is an MBD pattern obtained from another rod-sections. The hexagonal networks and matrix reflections are also observed in this figure. As shown in Figure 2(e), the hexagonal network rotates to 10 degrees from $[100]_m$ to $[\bar{1}\bar{2}10]_p$. In Figure 2(c), the angle between $[100]_m$ and $[\bar{1}\bar{2}10]_p$ is 15 degrees as shown in Figure 2(f). All rod-sections observed in this study could be classified into three types of angular relation, namely the angle between $[100]_m$ and $[\bar{1}\bar{2}10]_p$ is 0, 10 ± 3 and 15 degrees. We call them hereafter 0 deg. type, middle range type and 15 deg. type, respectively.

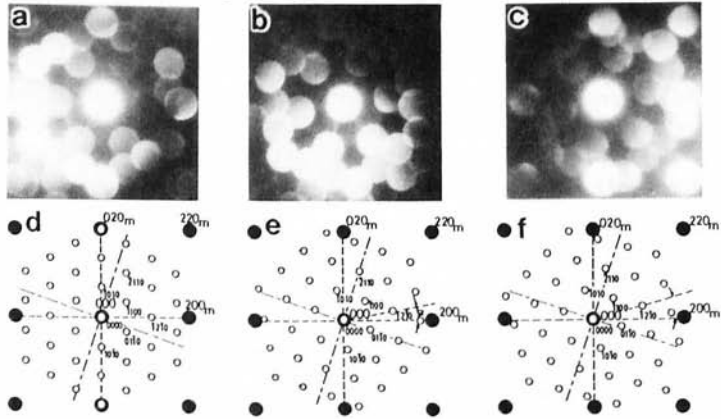


Figure 2. MBD patterns taken from the cross-sections of rod-shaped β' phase. (d), (e) and (f) are schematic illustrations of (a), (b) and (c), respectively.

Figure 3(a) is a selected area diffraction pattern taken from a normal direction of the longitudinal section of the β' phase. The diffraction spots from the matrix (\circ) and the β' phase (\bullet) are detected as shown in Figure 3(b). The diffraction spots from the β' phase are observed as a pair and are located between 000 and 020 matrix spots. In Figure 3(b), the ratio of the spacings a , b and c to spacing between 000 and 002 spots are $a=c=0.46$ and $b=0.08$. The rows of the diffraction spots are also observed at the mid-point between 000 and 002 spots. The plane spacings calculated from the distance between those rows of diffraction spots and 000 spot is 0.405nm [3]. Figures 3(c) and 3(e) are selected area diffraction patterns taken from other β' phase. The existence of a row of diffraction spots between 000 and 002 matrix spots in Figures 3(c) and 3(e) are similar to those shown in Figure 3(a). While in Figure 3(c), the spacing a , b , and c have the same value which is different from those of Figure 3(a). In Figure 3(e), the ratio of spacings a , b and c to the nearest distance between 000 and 200 diffraction spots are $a=c=0.17$ and $b=0.66$, respectively. The values are different from those of Figures 3(a) and 3(c). The spacings a , b and c are classified into three types as shown in Figures 3(b), 3(d) and 3(f). If three types of diffraction patterns are produced by the precipitates with rotating relationship with the matrix as shown in Figure 2, it is expected that the diffraction patterns obtained from the direction normal to the longitudinal direction of the rod-shaped β' phase have the spacings of the lattice planes of $\{\bar{1}\bar{2}10\}_p$, $\{1\bar{1}00\}_p$ and $\{\bar{1}\bar{3}\bar{2}0\}_p$.

The spacings of the lattice planes estimated from the spacing of $a+b$ in Figure 3(b), a in Figure 3(d) and $a+b$ in Figure 3(f) correspond to $\{1\bar{2}10\}_p$, $\{1\bar{1}00\}_p$ and $\{\bar{1}3\bar{2}0\}_p$, respectively. The spacings of $a+b$ in Figure 3(b), a in Figure 3(d) and $a+b$ in Figure 3(f) correspond to the plane spacings of $\{1\bar{2}10\}_p$, $\{1\bar{1}00\}_p$ and $\{\bar{1}3\bar{2}0\}_p$, respectively. It is interpreted that the rows of diffraction spots interposed between a and b in Figures 3(b) and 3(f) are the double diffraction spots between the matrix and β' phase.

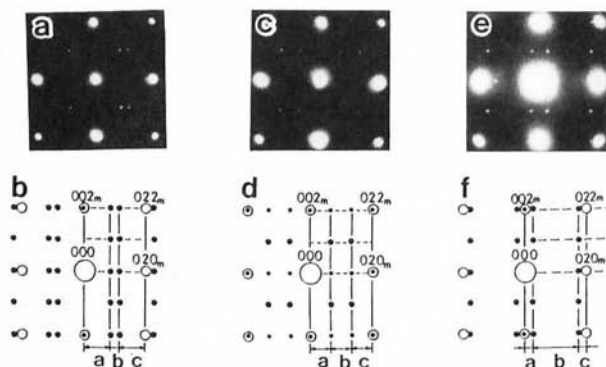


Figure 3. Selected area diffraction patterns taken from directions normal to the longitudinal direction of the rod-shaped β' phase. (b),(d) and (f) are schematic illustrations of (a), (c) and (e), respectively.

Crystal Structure of precipitate

Jacobs [3] assumed that the crystal lattice of the metastable β' phase in Al-Mg-Si alloy was a hexagonal one. But he did not determine the positions of Mg and Si atoms inside the β' phase. We assumed that the crystal structure was one as indicated in Figure 4 from the results of the present study. Thus, the crystal lattice is interpreted to be a H.C.P., not simple hexagonal, because the intensity of the 0001 diffraction spot is weak. And the lattice parameter of a -axis is 0.407nm as shows in Figure 1(b). Another reason is that the intensity of diffraction spots corresponding to the plane spacing of 0.35nm is stronger than that of 0.61nm in all MBD patterns as shown in Figure 2. A lattice parameter of c -axis is equal to that determined by Jacobs[3], $c=0.405\text{nm}$ and the chemical composition of the precipitates is estimated to be Mg:Si=2:1.

Figure 5 shows the diffraction patterns simulated based on the assumed crystal structure. Figure 5(a) is results of the pattern for the direction parallel to c -axis, [0001]. Figures 5(b) to (d) represent the patterns for the incident beam directions parallel to the A, B and C directions as shown in Figure 4, which are perpendicular to the c -axis. The direction A is tilted by 30 degrees around c -axis from the direction B. The direction C is tilted by 10.9 degrees around c -axis from the direction A (and tilted by 19.1 degrees around c -axis from the direction B). These results are in good agreement with the experimentally obtained diffraction patterns as shown in Figures 2 and 3. Figure 6 shows an observed H.R. image from a precipitate to compare with the simulated image based on the crystal structure as shown in Figure 4. The

agreement between the observed and simulated images (inserted in this figure) is also good.

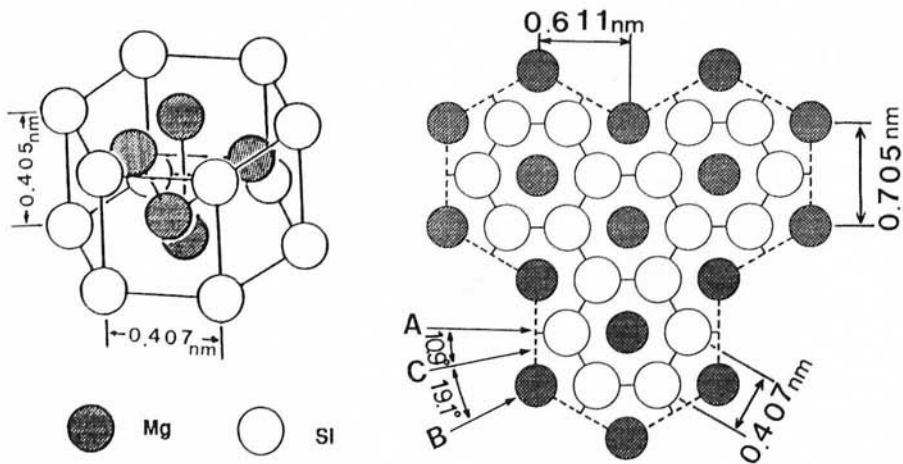


Figure 4. Schematic illustration of the crystal structure of the precipitate proposed in the present study.

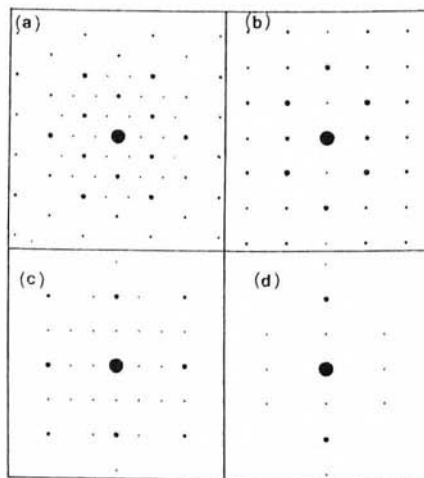


Figure 5. Simulated diffraction patterns for the crystal structure shown in Figure 4. (a) incident beam // $[0001]_p$. (b) incident beam // A, (c) incident beam // B and (d) incident beam // C. Directions A, B and C are shown in Figure 4.

EDX analysis

Figure 7 shows a result of EDX analysis obtained from the β' phase, extrapolated from Al atomic % of the matrix [6]. The composition of Mg and Si obtained from y-intercepts of Figures

7(a) and (b) are 62.7 atomic % and 37.3 atomic %, respectively. Therefore, the ratio of Mg/Si is about 1.68. Then the number of Si atoms in one unit cell assumed in Fig.4 must be increased to the 1.68 of Mg/Si ratio. It can be assumed that the single unit cell consists of 0.94Mg and 0.06Si. The diffraction patterns simulated by assuming the above structure are in good agreement with the results shown in Figure 5. Lynch et. al.[7] reported that the chemical composition of the β' phase in Al-Mg-Si alloys was Mg:Si=0.44:1. The simulated diffraction patterns based on the unit cell which has the chemical composition of Mg:Si=1:2 were similar to those shown in Figure 5. The changes in the ratio of Mg/Si is formed to have little influence on the diffraction pattern. Simulated H.R. images were not also affected by the change in the ratio of Mg/Si. This is because that the atomic scattering factors for electron beam of Mg and Si atoms are very close.

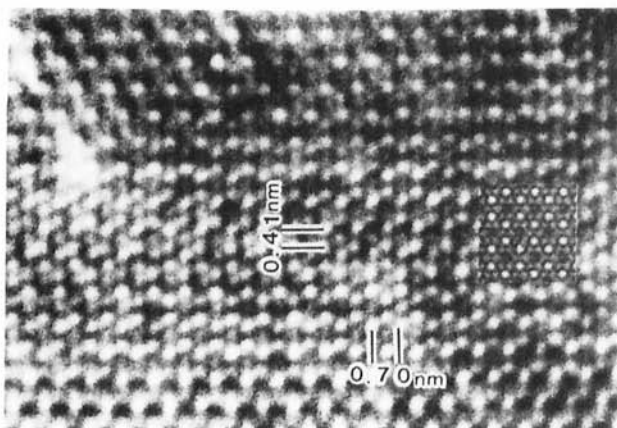


Figure 6. Typical high resolution image of the rod-section with a simulated image. (defocus $\Delta f = -30\text{nm}$, thickness of specimen = 64.8nm .)

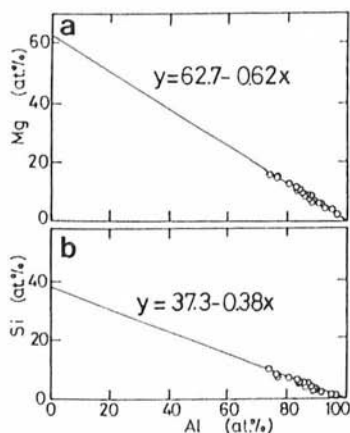


Figure 7. Chemical composition of the precipitates detected by EDX spectrometer. (a) Mg at.% versus Al at.% and (b) Si at.% versus Al at.%.

Conclusions

The rod-shaped β' phase in an aged Al-1.0mass%Mg₂Si alloy was observed by a transmission electron microscope in order to clarify the crystal structure. The obtained results are summarized as follows.

(1) The micro-beam diffraction (MBD) patterns obtained from the parallel direction to the longitudinal direction of the β' phase reveals the rotating relationships between the matrix $\langle 100 \rangle$ direction and the longitudinal direction of the β' phase. The rotating axis is parallel to the longitudinal direction of the β' phase.

(2) Three types of selected area diffraction patterns are obtained from the β' phase observed from the normal direction to their longitudinal direction and the parallel direction to the $\langle 100 \rangle$ matrix direction. These diffraction patterns are explained in terms of the rotating relationships between the matrix and the precipitates.

(3) Based on the obtained results, the crystal structure of the β' phase is proposed as follows: the crystal system is H.C.P. and its lattice parameters are $a=0.407\text{nm}$ and $c=0.405\text{nm}$. The simulated diffraction patterns and high resolution images based on the proposed crystal structure are in good agreement with the experimentally obtained diffraction patterns and high resolution images.

(4) The ratio of Mg/Si of the β' phase was determined to be 1.68 by the EDX analysis. The simulated diffraction patterns based on the proposed crystal structure of the β' phase having Mg/Si=1.68 were similar to those of Mg/Si=2.0.

References

1. Y. Komatsu et al., J. Japan Inst. Light Metals, 40, (1991), 276.
2. G. Thomas, J. Inst. Metals, 90, (1961-62), 57.
3. M. H. Jacobs, Phil. Mag., 26, (1972), 1.
4. K. Matsuda, S. Tada and S. Ikeno, J. Electron Microscopy, 42, (1993), 1.
5. K. Matsuda et al., J. Japan Light Metals, 43, (1993), 127.
6. T. Sato, J. Japan Light Metals, 42, (1992), 471.
7. J. P. Lynch, L. M. Brown and M. H. Jacobs, Acta Metall. 30, (1982), 1389.